

**NEW <sup>14</sup>C DETERMINATIONS FROM LAKE SUIGETSU, JAPAN: 12,000 TO 0 CAL BP**

Richard A Staff<sup>1,2</sup> • Christopher Bronk Ramsey<sup>1</sup> • Charlotte L Bryant<sup>3</sup> • Fiona Brock<sup>1</sup> • Rebecca L Payne<sup>4</sup> • Gordon Scholaut<sup>5</sup> • Michael H Marshall<sup>6</sup> • Achim Brauer<sup>5</sup> • Henry F Lamb<sup>6</sup> • Pavel Tarasov<sup>7</sup> • Yusuke Yokoyama<sup>8</sup> • Tsuyoshi Haraguchi<sup>9</sup> • Katsuya Gotanda<sup>10</sup> • Hitoshi Yonenobu<sup>11</sup> • Takeshi Nakagawa<sup>4</sup> • Suigetsu 2006 Project Members<sup>12</sup>

**ABSTRACT.** Calibration is a fundamental stage of the radiocarbon (<sup>14</sup>C) dating process if one is to derive meaningful calendar ages from samples' <sup>14</sup>C measurements. For the first time, the IntCal09 calibration curve (Reimer et al. 2009) provided an internationally ratified calibration data set across almost the complete range (0 to 50,000 cal BP) of the <sup>14</sup>C timescale. However, only the last 12,550 cal yr of this record are composed of terrestrial data, leaving approximately three quarters of the <sup>14</sup>C timescale necessarily calibrated via less secure, marine records (incorporating assumptions pertaining to the temporally variable “marine reservoir effect”). The predominantly annually laminated (varved) sediment profile of Lake Suigetsu, central Japan, offers an ideal opportunity to derive an extended terrestrial record of atmospheric <sup>14</sup>C across the entire range of the method, through pairing of <sup>14</sup>C measurements of terrestrial plant macrofossil samples (extracted from the sediment) with the independent chronology provided through counting of its annual laminations.

This paper presents new data (182 <sup>14</sup>C determinations) from the upper (largely non-varved) 15 m of the Lake Suigetsu (SG06) sediment strata. These measurements provide evidence of excellent coherence between the Suigetsu <sup>14</sup>C data and the IntCal09 calibration curve across the last ~12,000 cal yr (i.e. the portion of IntCal based entirely on terrestrial data). Such agreement demonstrates that terrestrial plant material picked from the Lake Suigetsu sediment provides a reliable archive of atmospheric <sup>14</sup>C, and therefore supports the site as being capable of providing a high-resolution extension to the “wholly terrestrial” (i.e. non-reservoir-corrected) calibration curve beyond its present 12,550 cal BP limit.

**INTRODUCTION**

Soon after the development of the radiocarbon dating technique in the mid-20th century (Libby et al. 1949; Libby 1955), it became apparent that a calibration stage was required if “radiocarbon time” were to be translated into a more meaningful representation of the passing of “real,” calendar time (de Vries 1958; Suess 1970). Such calibration is necessary because of temporal variation in the ambient atmospheric concentration of <sup>14</sup>C ( $\Delta^{14}\text{C}$ ), related to changes in the Earth's geomagnetic field intensity, changes in solar activity, and rearrangements of the distribution of carbon between the respective reservoirs of the global carbon cycle system.

Calibration is achieved through comparison of measured <sup>14</sup>C determinations with those of samples of known calendar age. To derive such a data set, a range of natural paleoenvironmental archives,

<sup>1</sup>Oxford Radiocarbon Accelerator Unit (ORAU), Research Laboratory for Archaeology and the History of Art (RLAHA), University of Oxford, Dyson Perrins Building, South Parks Road, Oxford OX1 3QY, United Kingdom.

<sup>2</sup>Corresponding author. Email: richard.staff@rlaha.ox.ac.uk.

<sup>3</sup>NERC Radiocarbon Facility–Environment (NRCF-E), Scottish Enterprise Technology Park, Rankine Avenue, East Kilbride G75 0QF, United Kingdom.

<sup>4</sup>Dept. of Geography, University of Newcastle, Newcastle-upon-Tyne NE1 7RU, United Kingdom.

<sup>5</sup>Section 5.2: Climate Dynamics and Landscape Evolution, German Research Center for Geoscience (GFZ), Telegrafenberg, D-14473 Potsdam, Germany.

<sup>6</sup>Institute of Geography and Earth Sciences, Aberystwyth University, Aberystwyth SY23 3DB, United Kingdom.

<sup>7</sup>Institute of Geological Sciences, Palaeontology, Freie Universität Berlin, Malteserstrasse 74-100, Building D, 12249 Berlin, Germany.

<sup>8</sup>Dept. of Earth and Planetary Sciences, Faculty of Science, University of Tokyo, 7-3-1 Hongo, Bunkyo-ku, Tokyo 113-0033, Japan. Also: Ocean Research Institute, University of Tokyo, 1-15-1 Minami-dai, Nakano-ku, Tokyo 164-8639, Japan.

<sup>9</sup>Dept. of Biology and Geosciences, Osaka City University, 3-3-138 Sugimoto, Japan.

<sup>10</sup>Faculty of Policy Informatics, Chiba University of Commerce, Chiba 272-8512, Japan.

<sup>11</sup>College of Education, Naruto University of Education, Naruto 772-8502, Japan.

<sup>12</sup>For full details, see: www.suigetsu.org.

providing records of  $\Delta^{14}\text{C}$  variation through time, has been exploited over recent decades. Such records must demonstrate a reliable, independent means of deriving calendar age, against which the  $^{14}\text{C}$  determinations can be directly compared. Dendrochronologically dated tree-ring data have been central to such efforts; however, such data are limited, at present, to the last 12,550 cal yr (Reimer et al. 2009), leaving approximately three quarters of the  $^{14}\text{C}$  timescale to be calibrated via alternative marine records. Since these marine data (demonstrated most extensively by Hughen et al. 2004, 2006 and Fairbanks et al. 2005) require correction for the temporally and spatially variable “marine reservoir effect” (Reimer and Reimer 2001), such approximations for  $\Delta^{14}\text{C}$  incorporate additional uncertainties. Similarly, speleothem data (e.g. Hoffmann et al. 2010) require a reservoir correction (for the “dead carbon fraction” from geologically old carbonate), which, like the marine correction, incorporates additional uncertainties. For a detailed discussion of the many alternative records for extending the  $^{14}\text{C}$  calibration curve further back in time, see, *inter alia*, Reimer et al. (2002) and van der Plicht et al. (2004), which additionally define the acceptance criteria of specific data sets into the consensus calibration curve, IntCal.

A “wholly terrestrial” (*sensu* Staff et al. 2009; i.e. with no need for reservoir correction) sequence of  $^{14}\text{C}$  data across the entire range of the radiocarbon dating method, beyond the existing limit of dendro-calibration, would remove these uncertainties associated with the marine records, and therefore remains a fundamental aim of the  $^{14}\text{C}$  community. The varved sedimentary record of Lake Suigetsu, Honshu Island, central Japan (35°35'N, 135°53'E), provides “a natural timekeeper” and faithful recorder of environmental change (Fukusawa 1995), including “a very exciting record of atmospheric  $^{14}\text{C}$  changes” spanning the complete range of the  $^{14}\text{C}$  dating method (Kitagawa and van der Plicht 2000). In this way, Lake Suigetsu provides an ideal opportunity to extend the wholly terrestrial  $^{14}\text{C}$  calibration curve back to the limit of  $^{14}\text{C}$  detection.

A previous study (Kitagawa and van der Plicht 1998a,b, 2000) obtained ~300  $^{14}\text{C}$  determinations from macrofossils (leaves, twigs, and insect fragments) extracted from a ~75-m sediment core (SG93) taken from Lake Suigetsu. However, problems with the varve-based calendar age scale of the SG93 record precluded the widespread adoption of the Suigetsu data set for calibration purposes (van der Plicht et al. 2004). A statistical re-analysis (Staff et al. 2010) of this SG93 data set highlighted that gaps between successively drilled sections of the SG93 sediment core were primarily responsible for the errors in the SG93 varve year age scale, while uncertainties in the varve counting itself represented a more minor, secondary cause.

In contrast, retrieval of multiple, overlapping sediment cores from Lake Suigetsu enabled complete recovery of the sediment profile for the present “Suigetsu Varves 2006” project (Nakagawa et al. 2011). Utilizing the composite 73.19-m sediment core (SG06) thus obtained, the Suigetsu Varves 2006 project seeks to exploit the excellent paleoenvironmental archive provided by the annually laminated sediment sequence more fully, including the generation of an improved  $^{14}\text{C}$  calibration data set.

This paper provides new  $^{14}\text{C}$  determinations from the upper 15 m of the SG06 sediment core, representing approximately the last 12,000 cal yr. Since this time period is represented in the consensus calibration curve, IntCal09 (Reimer et al. 2009), by a reliable, direct archive of past changes in atmospheric  $^{14}\text{C}$  (i.e. robustly cross-checked, dendrochronologically dated tree rings), this latter data set can be used to verify that terrestrial macrofossils present within the Lake Suigetsu sediment profile similarly represent a reliable record of past changes in  $\Delta^{14}\text{C}$ .

## METHODS

### Sediment Coring

Overlapping sections of sediment were obtained from 4 parallel boreholes (A, B, C, and D) such that material from any given Lake Suigetsu sedimentary horizon was represented by at least one of these individual sediment cores. The 4 boreholes were situated within 40 m horizontal distance of each other, at the lake's depocenter of 34 m. Through visual comparison of major event horizons (including tephra, flood layers, turbidite layers, and laminae with distinct coloration) between core sections from the 4 separate boreholes, a fully continuous composite core (SG06) of 73.19 m length was produced, spanning at least the last 150 kyr (Nakagawa et al. 2011). Continuity of the sedimentary facies can clearly be seen through visual comparison of the characteristic event layers from equivalent depths across the separate cores. A more thorough account of the sediment coring process, as well as a description of the SG06 core stratigraphy, is given in Nakagawa et al. (2011).

### Macrofossil Sampling

Macrofossil samples were hand-picked from the exposed surface of the sediment, after longitudinal division of the cores (Figure 1). The majority of samples were tree leaves, although small twigs, bark, seeds, and a few segments of insects were also present (Staff 2011). Sampling was thus undertaken throughout the time period of interest for  $^{14}\text{C}$  calibration (i.e. back to about 60,000 cal BP, at approximately 42 m composite depth).

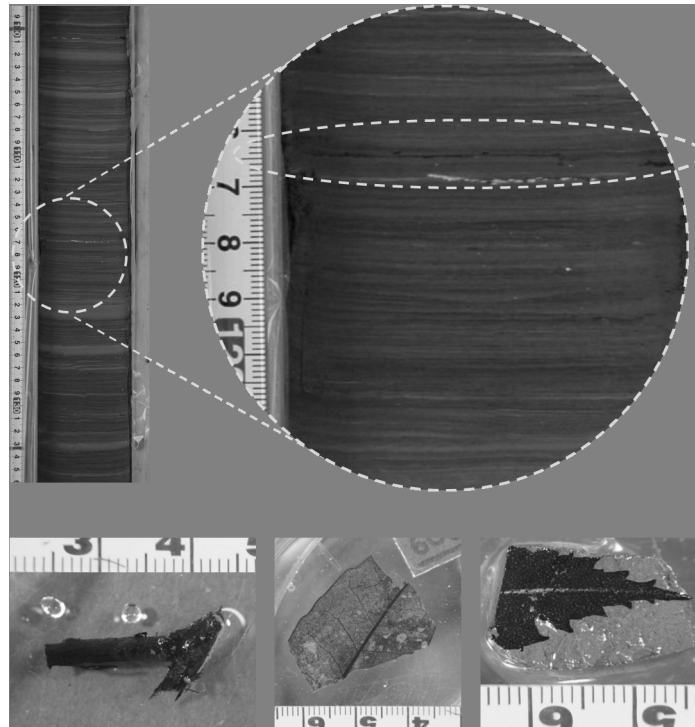


Figure 1 Illustration of the visual identification of macrofossils within the SG06 sediment core from examination of the exposed sediment surface generated through longitudinal division of the cores. Three illustrative examples of plant macrofossil samples extracted from SG06 (a twig, evergreen broad leaf, and deciduous broad leaf) are also shown.

“Event layers” (i.e. layers attributed to flood or turbidite events; Nakagawa et al. 2011) were avoided for sampling, despite the fact that they might have contained quite tempting macrofossil samples. Macrofossils washed into the lake at times of flooding bear an increased risk of having been held *in situ* elsewhere in the lake catchment prior to in-wash, and would therefore contain an inbuilt age as compared to the date of the event layer formation itself. Similarly, samples contained within turbidite layers (whether caused by earthquake activity or otherwise) are likely to have been reworked from material previously stored in the upper littoral zone of the lake sediments, and could again provide material with an inbuilt age (Hajdas et al. 1995).

Macrofossil samples from the outer edge of the sediment core were not analyzed, since these samples might potentially have been moved up or down the sediment column during the coring process. Also, samples from the upper 5 cm of core sections were avoided because of the potential for these layers to have been compacted/disturbed during the core extraction process (Nakagawa et al. 2011). Thus, only samples taken from a sound chronostratigraphic context were obtained for dating.

Intact pieces of single terrestrial macrofossils were chosen for analysis since such samples are far less likely to have moved up or down the sediment profile as compared to an unidentifiable mixture of organic remains, which, in general, would be far less reliable for dating. Such a mixture of sampling material might represent a range of differing  $^{14}\text{C}$  ages, and therefore not be appropriate for combining into a single sample for dating (Hatté and Jull 2007).

Since the strength of the Lake Suigetsu macrofossil record for  $^{14}\text{C}$  calibration purposes lies in the fact that samples are of terrestrial species, samples identified as aquatic species (those growing within the lake itself) were necessarily avoided for dating. Such samples might be expected to demonstrate an offset from the contemporaneous atmospheric  $^{14}\text{C}$  record as a result of lake reservoir effects (Walker 2005:29–30).

Broad leaves were preferentially sampled over seeds, needles, twigs, or bark on the assumption that since the leaf samples are generally much more fragile, they would be more likely to have been transported relatively quickly between their separation from the living organism and their deposition in the anoxic basal lake sediments if they were to remain intact enough to yield sufficient carbon (ideally  $>0.6$  mg C) for  $^{14}\text{C}$  dating. This rapid transfer of sample material is essential if inbuilt  $^{14}\text{C}$  ages of samples (as compared to the timing of the sedimentation event itself) are to be avoided. Observation of the aerobic decomposition of leaves in the temperate terrestrial environment suggests that this time lag from host organism to deposition in the lake varves must be relatively short (i.e. well below the resolution of the calibration data set being produced from the project) if leaves are to survive intact enough to meet this minimum mass criterion. This approach of selecting “fragile macrofossils” is advocated by Hatté and Jull (2007), who suggest that such samples would also be damaged/destroyed by sediment reworking.

Although very scarce in the lake record anyway, insects were preferentially avoided for dating since the synthesis of  $^{14}\text{C}$  via the trophic pathway into these organisms is not as direct (from the atmosphere) as is the case with photosynthesizing terrestrial plants. Detrital feeders, for example, might feed on relatively old, decaying organic material, and assimilate this relatively older carbon (depleted in  $^{14}\text{C}$ ) into their tissue, again producing inbuilt  $^{14}\text{C}$  ages.

### **Radiocarbon Dating**

The terrestrial macrofossil samples were washed repeatedly with ultrapure (Milli-Q™, Millipore) water upon subsampling from the core, and subsequently stored in dilute hydrochloric acid (HCl;

~0.2M) to minimize the potential for contamination from modern atmospheric carbon during transport and storage. Samples were subsequently selected for <sup>14</sup>C dating according to their stratigraphic position, sample type, and sample size (following the provisos outlined above).

The samples selected for dating were divided between the Oxford Radiocarbon Accelerator Unit (ORAU) and NERC Radiocarbon Facility-Environment (NRCF-E), East Kilbride, laboratories such that the total number of samples to be dated at each lab (~300) was evenly distributed across the time period represented by the <sup>14</sup>C dating method (about 0 to 60,000 cal BP; SG06 composite core depths 0 to ~42 m). As a method of quality assurance, ~10% interlaboratory duplication of (sufficiently large) samples was targeted as a means of demonstrating the comparability of data between the 2 labs. Again, these samples were divided as regularly as possible down the sediment profile.

Sample pretreatment for accelerator mass spectrometry (AMS) <sup>14</sup>C dating followed standard acid-base-acid (ABA; occasionally referred to elsewhere as “acid-alkali-acid” or AAA) methodologies, according to the regular laboratory protocols of both labs (Table 1). Likewise, subsequent sample combustion, graphitization, and target pressing for AMS were performed according to the standard laboratory protocols of the respective facilities (Table 1).

Table 1 The chemical pretreatment, combustion, and graphitization protocols of the Oxford Radiocarbon Accelerator Unit (ORAU) and NERC Radiocarbon Facility-Environment (NRCF-E) laboratories applied to the SG06 plant macrofossil samples presented herein.

	ORAU protocol	NRCF-E protocol
Pretreatment (acid-base-acid, ABA)	1M HCl (20 min at 80 °C); 0.2M NaOH (20 min at 80 °C); 1M HCl (1 hr at 80 °C); Additional bleaching stage (5% wt:vol pH 3 NaClO <sub>2</sub> for ≤30 min) applied to sturdiest (twig and bark) samples (Brock et al. 2010)	1M HCl (30 min at 80 °C); 0.2M KOH (20 min at 80 °C); 1M HCl (1 hr at 80 °C)
Combustion	Samples freeze-dried and weighed into Sn capsules; combustion at 1000 °C (Brock et al. 2010)	Placed wet into Ag foil and freeze-dried; combustion in presence of CuO (Boutton et al. 1983)
Graphitization	H reduction of CO <sub>2</sub> to pure C (graphite) over an Fe catalyst (Vogel et al. 1984) for 6 hr at 560 °C (Dee and Bronk Ramsey 2000)	Reduction to CO over Zn (at 425 °C), prior to further reduction over Fe (18 hr at 610 °C) to elemental C (graphite; Slota et al. 1987)

Samples at ORAU were dated on the HVEE AMS system (described in Bronk Ramsey et al. 2004), while samples at NRCF-E (hosted by the Scottish Universities Environmental Research Centre, SUERC) were dated on either the National Electrostatics Corporation (NEC) 5MV tandem AMS or the NEC 250kV single-stage AMS (SSAMS) systems (Xu et al. 2004; Freeman et al. 2010; Naysmith et al. 2010).

A size-dependent background correction, equivalent to the addition of  $1.6 \pm 0.8$  µg of modern carbon per sample, was allowed for, in addition to the standard background corrections made at the individual laboratories. This value was estimated independently for both labs' data sets, based upon the size-dependence of measurements on samples from the lower (varved) portion of the SG06 core. The fact that the derived background correction is identical for both labs suggests that it is characteristic of the specific core and sampling methodologies applied.

### Statistical Methods

As introduced above, the purpose of this paper is to examine the reliability of the plant macrofossil samples extracted from the Lake Suigetsu sediment profile as reflecting the contemporaneous atmospheric radiocarbon concentration ( $\Delta^{14}\text{C}$ ). A robust, wholly terrestrial comparison data set (the consensus calibration curve, IntCal09; Reimer et al. 2009) is, at present, only available for the last 12,550 cal yr. Therefore, the data presented here pertain only to this time period demonstrating direct comparison of atmospheric data.

To assess the concordance of the respective data sets, the SG06  $^{14}\text{C}$  data were calibrated against the IntCal09 calibration curve (Reimer et al. 2009) using a *P\_Sequence* deposition model in the Bayesian software, OxCal (v 4.1; Bronk Ramsey 2008, 2009a; <https://c14.arch.ox.ac.uk/oxcal/OxCal.html>). A *P\_Sequence* model was applied, since it provides the most realistic depiction of lacustrine sedimentation, with the complexity (randomness) of the underlying sediment deposition modeled according to a Poisson process.

Countable varves are only present in SG06 from 1250.0 to 4601.4 cm composite depth (about 10,000 to 60,000 cal BP; Nakagawa et al. 2011), so varve count data are not included in the model. Instead, “event-free depth” (cf. the “event-removed” sediment profile of Katsuta et al. 2007) is used within the deposition sequence. This event-free depth scale is based upon the composite depth model, but excludes instantaneous deposits in excess of 5 mm thickness (representing individual flood, earthquake, or tephra events, for example). Such a depth scale allows more robust age modeling than if such large, individual events were included, but is less robust than if the full interannual variability (of varve thickness information) were able to be included.

The rigidity of the *P\_Sequence*, i.e. the *k* parameter in OxCal, was derived according to Eq. A.17 of Bronk Ramsey (2008) to equal  $2\text{ cm}^{-1}$ , based upon an assumed fractional uncertainty at the midpoint of a known-duration core section of 3.5%. Comparison with varve count data from lower down the sediment profile suggests that such a value is representative of the down-core variations of deposition rate in SG06.

A uniform prior probability distribution of 750 to  $-50$  cal BP was applied to the upper Boundary of the model (the “core top”), while an additional Boundary was inserted at 175.0 cm event-free depth (to account for the empirically observed change in deposition rate of the uppermost sediment section). No additional prior chronological information was applied to the lower Boundary of the model (“1500.0 cm composite depth”). Other than the model resolution being set to 1 yr, all modeling parameters were the same as the OxCal default settings.

An *r-type* outlier model was implemented (Bronk Ramsey 2009b; Bronk Ramsey et al. 2010), with all  $^{14}\text{C}$  determinations (*R\_F14C*) and *R\_Combine* given an equal (0.05) prior probability of being outliers (with the latter, *R\_Combine* parameter combining the duplicated measurements from specific depth horizons). The *r-type* outlier model was chosen since this specification allows for short-term fluctuations in the  $^{14}\text{C}$  concentrations between the respective  $^{14}\text{C}$  reservoirs of the sample data (from Lake Suigetsu) and the calibration curve (IntCal09) data sets.

In total, 182  $^{14}\text{C}$  determinations were included in the model (92 from ORAU and 90 from NRCF-E), representing 160 separate SG06 depth horizons. These 160 dated macrofossils consisted of 90 deciduous broad leaf samples, 59 evergreen broad leaves, 8 small twigs, and 3 bark samples. Additionally, the model included “date” query functions at the positions of the “SG06-1288” tephra horizon (at 1286.1 to 1288.0 cm composite depth, 1273.4 cm event-free depth; Smith et al. 2011) and of the “Holocene onset” in SG06 (at 1436.4 cm composite depth, 1413.4 cm event-free depth,



as identified from the multiple paleoenvironmental proxy data obtained by Suigetsu Varves 2006 project members). A truncated version of the model coding for this Poisson process deposition model is provided in Appendix 1.

## RESULTS

The 182  $^{14}\text{C}$  determinations of terrestrial plant macrofossil samples picked from the upper 15 m (composite depth) of the SG06 sediment core are given in Appendix 2. All of these data were included in the OxCal P\_Sequence model (described above). Figure 2 illustrates the fit of these data on to the IntCal09 calibration curve (Reimer et al. 2009), while Figure 3 demonstrates the relatively linear modeled deposition rate across this upper section of the Lake Suigetsu sediment profile. The results of the model fit show excellent agreement between the SG06 data and the IntCal09 calibration curve, with only 6 SG06  $^{14}\text{C}$  determinations identified as demonstrating  $\geq 95\%$  posterior probability of being outliers (with a further 7 samples demonstrating  $\geq 50\%$  posterior probability of being outliers). The probability density functions (PDFs) of the additional modeled query functions (the SG06-1288 tephra and Holocene onset) are shown in Figures 4 and 5, respectively.

## DISCUSSION

As illustrated in Figure 2, the degree of concordance between the respective atmospheric  $^{14}\text{C}$  data sets of the IntCal09 calibration curve (Reimer et al. 2009) and the Lake Suigetsu terrestrial plant macrofossils is excellent. Such agreement would be demonstrated yet further if the contributing data to the consensus calibration curve were additionally plotted, since the “smoothed” calibration curve masks a certain proportion of higher frequency variation in  $\Delta^{14}\text{C}$ . Since the majority of the Suigetsu data presented (149 of the total 160 dated macrofossil samples) were deciduous broad leaves (representing a single growth season) or evergreen broad leaves (representing  $\leq 3$  years’ growth), these samples would also be expected to represent additional higher frequency  $\Delta^{14}\text{C}$  variation than the time-integrated signal of the mostly decadal tree-ring blocks comprising the IntCal09 data set.

It could be argued that the fitting of one  $^{14}\text{C}$  data set on to that of the other might “force” agreement between the respective data sets. Firstly, the relative linearity of the modeled age-depth profile (Figure 3) provides additional support for the robustness of the derived calibrated timescale, since the sediment deposition rate is not allowed to vary to such an extent that the concordance of the data sets is forced (i.e. a relatively conservative value of  $\kappa = 2 \text{ cm}^{-1}$  is applied). Secondly, there is no *a priori* physical reason to suggest that the 2 data sets would not be in close agreement, since the IntCal curve and Lake Suigetsu data are both representative of direct  $^{14}\text{C}$  data from the atmosphere of the mid-latitude Northern Hemisphere (which is presumed to be thoroughly mixed, at least at the temporal resolution examined herein; Stuiver 1982). As highlighted above, the low number of SG06  $^{14}\text{C}$  determinations identified as being statistical outliers confirms the goodness of fit between these 2 terrestrial data sets.

The modeled age of the SG06-1288 tephra (commonly referred to elsewhere as the “U-Oki” tephra) is 10,231 to 10,202 cal BP (at the 68.2% probability range; 10,255 to 10,177 cal BP at the 95.4% probability range; Figure 4). Recently, Smith et al. (2011) geochemically correlated this tephra to its proximal volcanic source material, the U4 unit of Ulleungdo stratovolcano, South Korea (~500 km west-northwest of Lake Suigetsu). Furthermore, these authors were able to argon/argon ( $^{40}\text{Ar}/^{39}\text{Ar}$ ) date these proximal volcanic deposits to  $10,000 \pm 300$  cal yr BP, which is statistically indistinguishable from the  $^{14}\text{C}$ -derived age at  $1\sigma$  uncertainty. Thus, an independent verification is provided for the accuracy of the  $^{14}\text{C}$  chronology of this uppermost SG06 sediment section.

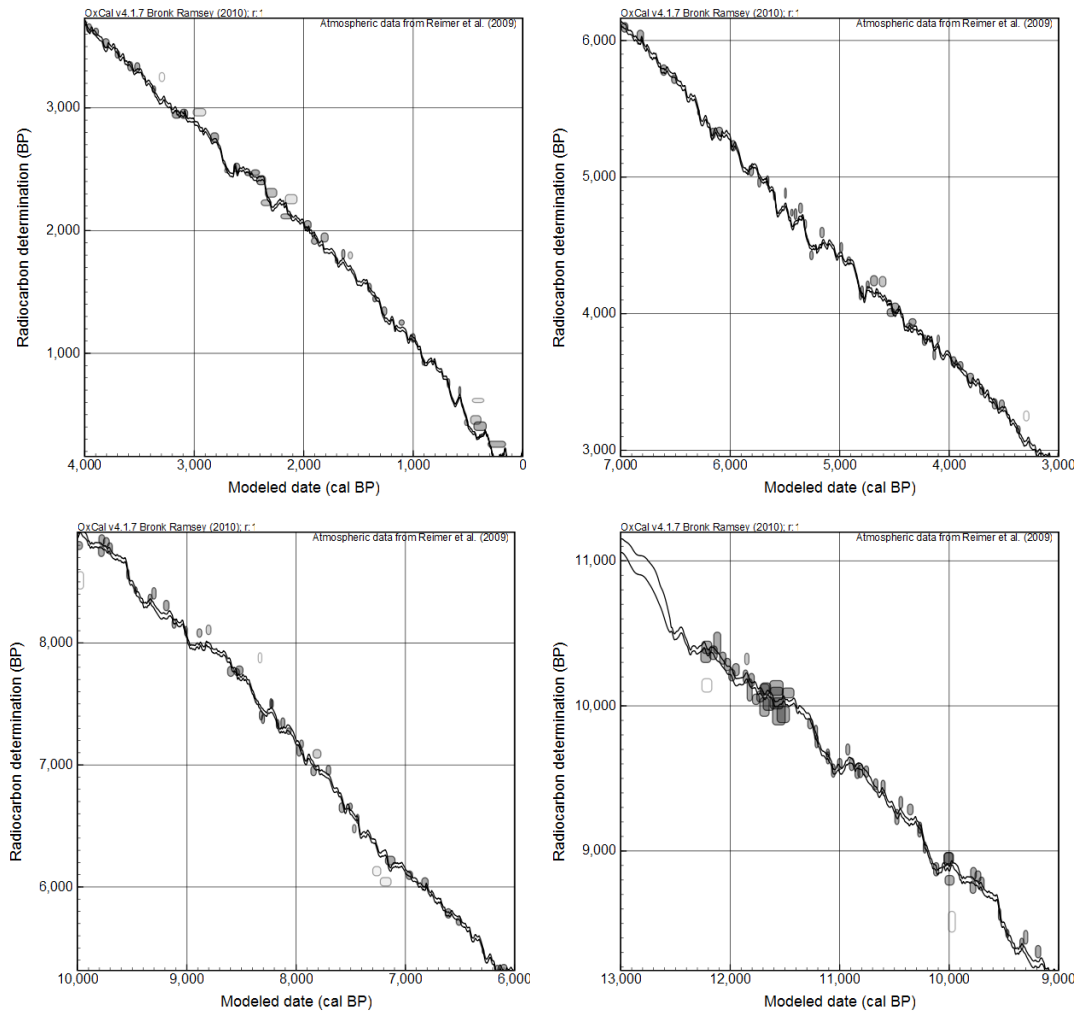


Figure 2 Illustration of the fit of the SG06 plant macrofossil  $^{14}\text{C}$  data on to the IntCal09 calibration curve (Reimer et al. 2009). For clarity, both the Lake Suigetsu data and IntCal09 calibration curve are shown at  $1\sigma$  uncertainty/68.2% probability ranges. The modeled data are shaded according to their posterior outlier probability, ranging from darker gray (0% posterior outlier probability) to white (100% probability).

The modeled age derived for the Holocene onset is 11,663 to 11,621 and 11,589 to 11,555 cal BP (at the 68.2% probability range; 11,671 to 11,538 cal BP at the 95.4% probability range; Figure 5). This age is also in good agreement with the age of the climatic transition (11,703 cal yr b2k, 11,653 cal yr BP; maximum counting error 99 yr) as defined in its principal Global Stratotype Section and Point (GSSP), the North Greenland Ice-core Project (NGRIP) record (Rasmussen et al. 2006; Walker et al. 2009). However, Muscheler et al. (2008) suggest that a downward revision of 65 yr to the NGRIP chronology is necessary, which, if indeed justified, would still leave the ages of the Holocene onset, as defined by the 2 respective paleoclimatic archives, in good agreement. The Suigetsu age is also in good agreement with the onset of the Holocene in the Meerfelder Maar (Germany) varve chronology of Brauer et al. (1999) at 11,590 cal BP. Thus, this paleoclimatic event provides further support for the reliability of the  $^{14}\text{C}$ -derived chronology presented here. It should be



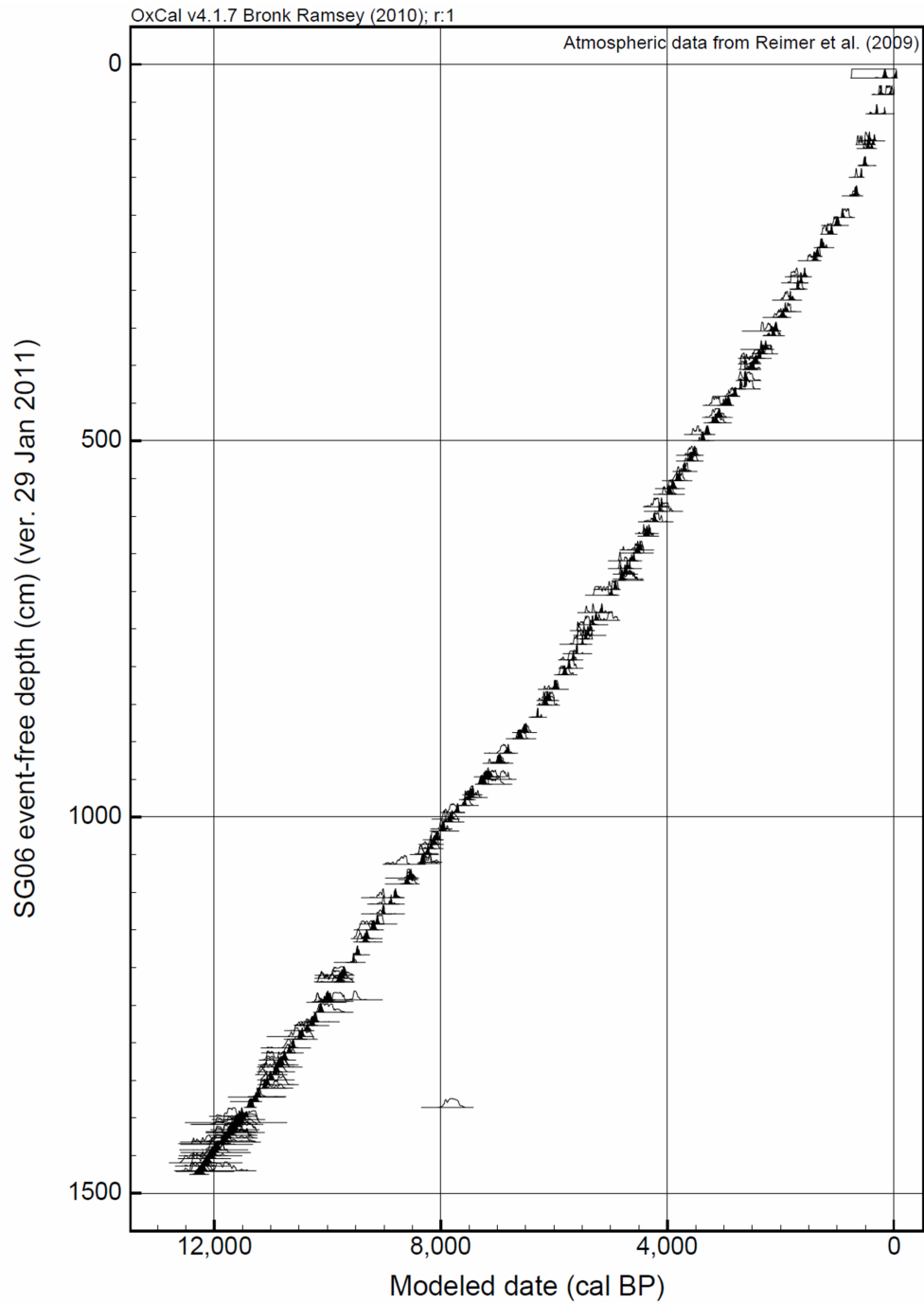


Figure 3 The relatively linear modeled deposition rate across the upper 15 m (composite depth; 14.77 m event-free depth) of the Lake Suigetsu (SG06) sediment profile. The posterior probability density functions (PDFs; darker shading) are shown overlying the prior, unmodeled PDFs (lighter shading).

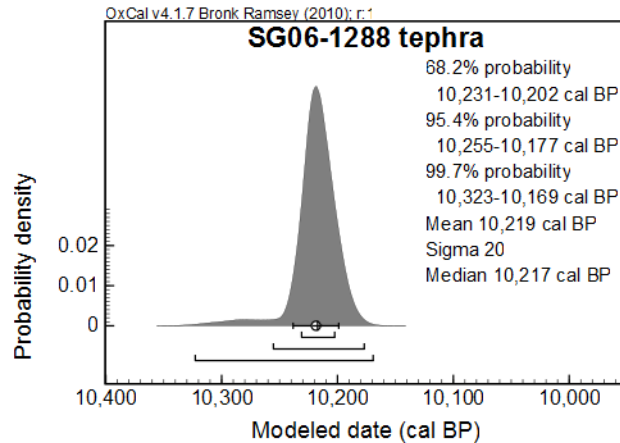


Figure 4 The posterior probability density function (PDF) generated for the SG06-1288 tephra horizon at 1286.1–1288.0 cm composite depth (1273.4 cm event-free depth).

emphasized that the climate signal of Greenland, central Europe, and Japan may not be synchronous at subcentennial timescales (indeed, one of the principal aims of the Suigetsu Varves 2006 project is to examine whether any such leads and lags are evident in the global climate system), so this comparison is made here for assessment of the broad reliability of the core's  $^{14}\text{C}$  data only. Furthermore, the age for the Holocene onset in SG06 presented here does not provide the “definitive” SG06 age for this event, as a more robust chronology for SG06 below 1250.0 cm composite depth will be enabled through incorporation of the forthcoming varve count data, which will significantly enhance the precision of the core's chronology below this depth. Instead, the  $^{14}\text{C}$ -derived age presented here will provide corroboration for the principal SG06 varve year chronology only.

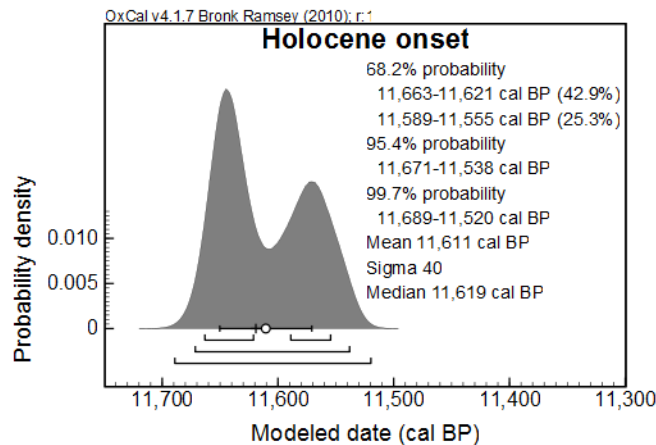


Figure 5 The posterior probability density function (PDF) generated for the placement of the Holocene onset in SG06 at 1436.4 cm composite depth (1413.4 cm event-free depth).

Unlike the present (Suigetsu Varves 2006) project, the previous study (Kitagawa and van der Plicht 1998a,b, 2000) did not carry out as many  $^{14}\text{C}$  measurements on macrofossils dating from the

Holocene, since the primary aim of that project was the extension of the calibration curve back in time from the then limits of calibration (11,390 cal BP from tree-ring data, extending to 21,950 cal BP with lower-resolution coral data; Stuiver and Reimer 1993). The additional <sup>14</sup>C analysis performed for the present project, extending through the later time period, serves (i) to provide greater confidence in the stratigraphic integrity (lack of sedimentary hiatuses) of the Lake Suigetsu sediment profile through demonstration of the coherence of its <sup>14</sup>C-derived chronology with alternative, reliable terrestrial calibration data; and (ii) to provide the chronology required for the additional, paleoenvironmental aims of the Suigetsu Varves 2006 project above the upper limit of countable varves. The former point has been demonstrated in this paper, supporting the integrity of the SG06 sediment core, and therefore provides support for the <sup>14</sup>C calibration and paleoenvironmental data sets to be produced from the lower core depths, preceding the present terrestrial limit of IntCal. The latter point is important for other goals of the Suigetsu Varves 2006 project, including investigation of the enigmatic “8.2 ka event,” as well as other paleoclimatic study from the upper 1250.0 cm of the SG06 core.

One final point to make is that, while the present paper has focused on the last ~12,000 cal yr (i.e. almost entirely representing the Holocene), the extension to the atmospheric <sup>14</sup>C calibration curve is required back into the Late Glacial. In Suigetsu, this period is represented by a lower average sedimentation rate (Kitagawa and van der Plicht 1998a,b), as well as reduced abundance of deposited plant macrofossil samples, which are both issues to be considered for the preceding time period, and will be more thoroughly discussed in future publications.

## **CONCLUSION**

Some 182 new <sup>14</sup>C determinations have been produced from the upper 15 m of the Lake Suigetsu (SG06) sediment core. Bayesian modeling of these data against the IntCal09 calibration curve (Reimer et al. 2009) has demonstrated the concordance of the respective data sets, which, across the time period covered (i.e. the last ~12,000 cal yr), are both represented by “wholly terrestrial” archives of atmospheric <sup>14</sup>C concentration, not incorporating any additional uncertainties associated with reservoir corrections. Therefore, the plant macrofossil samples extracted from the Lake Suigetsu benthic sediment profile are demonstrated as reliably representing past changes in atmospheric <sup>14</sup>C concentration, which provides support for the <sup>14</sup>C data to be produced from lower down the SG06 core, beyond the present limit of tree-ring-derived data in IntCal09. It is therefore believed that Lake Suigetsu, demonstrating annual laminations (varves) across the remainder of the <sup>14</sup>C dating technique, will provide a reliable, direct record of atmospheric <sup>14</sup>C data back to the detection limit of the <sup>14</sup>C method. Finally, it is hoped that such a data set will contribute significantly to future revisions of the consensus calibration curve, IntCal.

## **ACKNOWLEDGMENTS**

The authors would like to thank the UK Natural Environment Research Council (NERC; grants: NE/D000289/1 and NE/F003048/1, and NERC Radiocarbon Facility allocation 1219.0407), the Deutsche Forschungsgemeinschaft (DFG; grant: TA-540/3-1), and MEXT-Japan KAKENHI (grant: 21101002) for funding of the Suigetsu Varves 2006 project. Additionally, R S would like to thank RLAHA, University of Oxford for personal funding of his DPhil research (upon which the majority of this work is based), and the John Fell OUP Research Fund for financial support in the writing-up of papers stemming from this work. We thank members of the <sup>14</sup>C groups at ORAU, NRCF-E, and SUERC for their laboratory work and technical support in the production of the <sup>14</sup>C data presented, with especial thanks to Martin Humm and Philip Leach (ORAU), and Margaret Currie, Frank

Elliott, Callum Murray, and Liam Chalmers (NRCF-E). Finally, our sincerest thanks to Hiroyuki Kitagawa and Johannes van der Plicht for their pioneering work at Lake Suigetsu, and for providing the inspiration for the present project.

## REFERENCES

- Boutton TW, Wong WW, Hachey DL, Lee LS, Cabrera MP, Klein PD. 1983. Comparison of quartz and Pyrex tubes for combustion of organic samples for stable carbon isotope analysis. *Analytical Chemistry* 55(11): 1832–3.
- Brauer A, Endres C, Günter C, Litt T, Stebich M, Negen-dank JFW. 1999. High resolution sediment and vege-tation responses to Younger Dryas climate change in varved lake sediments from Meerfelder Maar, Ger-many. *Quaternary Science Reviews* 18(3):321–9.
- Brock F, Higham T, Ditchfield P, Bronk Ramsey C. 2010. Current pretreatment methods for AMS radiocarbon dating at the Oxford Radiocarbon Accelerator Unit (ORAU). *Radiocarbon* 52(1):103–12.
- Bronk Ramsey C. 2008. Deposition models for chrono-logical records. *Quaternary Science Reviews* 27(1–2): 42–60.
- Bronk Ramsey C. 2009a. Bayesian analysis of radiocar-bon dates. *Radiocarbon* 51(1):337–60.
- Bronk Ramsey C. 2009b. Dealing with outliers and off-sets in radiocarbon dating. *Radiocarbon* 51(3):1023–45.
- Bronk Ramsey C, Higham T, Leach P. 2004. Towards high-precision AMS: progress and limitations. *Radiocarbon* 46(1):17–24.
- Bronk Ramsey C, Dee M, Lee S, Nakagawa T, Staff RA. 2010. Developments in the calibration and modeling of radiocarbon dates. *Radiocarbon* 52(2–3):953–61.
- de Vries HL. 1958. Variation in concentration of radio-carbon with time and location on Earth. *Proceedings of the Koninklijke Nederlandse Akademie van Weten-schappen B* 61:94–102.
- Dee M, Bronk Ramsey C. 2000. Refinement of graphite target production at ORAU. *Nuclear Instruments and Methods in Physics Research B* 172(1–4):449–53.
- Fairbanks RG, Mortlock RA, Chiu T-C, Cao L, Kaplan A, Guilderson TP, Fairbanks TW, Bloom AL, Grootes PM, Nadeau M-J. 2005. Radiocarbon calibration curve spanning 0 to 50,000 years BP based on paired  $^{230}\text{Th}/^{234}\text{U}/^{238}\text{U}$  and  $^{14}\text{C}$  dates on pristine corals. *Qua-ternary Science Reviews* 24(16–17):1781–96.
- Freeman SPHT, Cook GT, Dougans AB, Naysmith P, Wilcken KM, Xu S. 2010. Improved SSAMS perfor-mance. *Nuclear Instruments and Methods in Physics Research B* 268(7–8):715–7.
- Fukushima H. 1995. Non-glacial varved lake sediment as a natural timekeeper and detector on environmental changes. *The Quaternary Research* 34(3):135–49. In Japanese with English abstract.
- Hajdas I, Bonani G, Goslar T. 1995. Radiocarbon dating the Holocene in the Gościąg Lake floating varve chro-nology. *Radiocarbon* 37(1):71–4.
- Hatté C, Jull AJT. 2007. Radiocarbon dating: plant mac-rofossils. In: Elias S, editor. *Encyclopedia of Quater-nary Science*. Amsterdam: Elsevier. p 2958–65.
- Hoffmann DL, Beck JW, Richards DA, Smart PL, Singa-rayer JS, Ketchmark T, Hawkesworth CJ. 2010. To-wards radiocarbon calibration beyond 28 ka using speleothems from the Bahamas. *Earth and Planetary Science Letters* 289(1–2):1–10.
- Hughen KA, Lehman SJ, Southon JR, Overpeck JT, Mar-chal O, Herring C, Turnbull J. 2004.  $^{14}\text{C}$  activity and global carbon cycle changes over the past 50,000 years. *Science* 303(5655):202–7.
- Hughen KA, Southon JR, Lehman SJ, Bertrand C, Turn-bull J. 2006. Marine-derived  $^{14}\text{C}$  calibration and activ-ity record for the past 50,000 years updated from the Cariaco Basin. *Quaternary Science Reviews* 25(23–24):3216–27.
- Katsuta N, Takano M, Kawakami S-I, Togami S, Fuku-sawa H, Kumuzawa M, Yasuda Y. 2007. Advanced micro-XRF method to separate sedimentary rhythms and event layers in sediments: its application to lacustrine sediment from Lake Suigetsu, Japan. *Journal of Paleolimnology* 37(2):259–71.
- Kitagawa H, van der Plicht J. 1998a. Atmospheric radio-carbon calibration to 45,000 yr B.P.: late glacial fluctu-ations and cosmogenic isotope production. *Science* 279(5354):1187–90.
- Kitagawa H, van der Plicht J. 1998b. A 40,000-year varve chronology from Lake Suigetsu, Japan: exten-sion of the  $^{14}\text{C}$  calibration curve. *Radiocarbon* 40(1): 505–15.
- Kitagawa H, van der Plicht J. 2000. Atmospheric radio-carbon calibration beyond 11,900 cal BP from Lake Suigetsu laminated sediments. *Radiocarbon* 42(3): 369–80.
- Libby WF. 1955. *Radiocarbon Dating*. 2nd edition. Chi-cago: University of Chicago Press.
- Libby WF, Anderson EC, Arnold JR. 1949. Age determi-nation by radiocarbon content: world-wide assay of natural radiocarbon. *Science* 109(2827):227–8.
- Muscheler R, Kromer B, Björck S, Svensson A, Friedrich M, Kaiser KF, Southon J. 2008. Tree rings and ice cores reveal  $^{14}\text{C}$  calibration uncertainties during the Younger Dryas. *Nature Geoscience* 1:263–7.
- Nakagawa T, Gotanda K, Haraguchi T, Danhara T, Yonenobu H, Brauer A, Yokoyama Y, Tada R, Take-mura K, Staff RA, Payne R, Bronk Ramsey C, Bryant C, Brock F, Schlögl G, Marshall M, Tarasov P, Lamb H, Suigetsu 2006 Project Members. 2011. SG06, a fully continuous and varved sediment core from Lake

- Suigetsu, Japan: stratigraphy and potential for improving the radiocarbon calibration model and understanding of late Quaternary climate changes. *Quaternary Science Reviews*. doi:10.1016/j.quascirev.2010.12.013.
- Naysmith P, Cook GT, Freeman SPHT, Scott EM, Anderson R, Xu S, Dunbar E, Muir GKP, Dougans A, Wilcken K, Schnabel C, Russell N, Ascough PL, Maden C. 2010.  $^{14}\text{C}$  AMS at SUERC: improving QA data with the 5MV tandem and 250kV SSAMS. *Radiocarbon* 52(2–3):263–71.
- Rasmussen SO, Andersen KK, Svensson AM, Steffensen JP, Vinther BM, Clausen HB, Siggaard-Andersen M-L, Johnsen SJ, Larsen LB, Dahl-Jensen D, Bigler M, Röthlisberger R, Fischer H, Goto-Azuma K, Hansson ME, Ruth U. 2006. A new Greenland ice core chronology for the last glacial termination. *Journal of Geophysical Research* 111:D06102, doi:10.1029/2005JD006079.
- Reimer PJ, Reimer RW. 2001. A marine reservoir correction database and on-line interface. *Radiocarbon* 43(2A):461–3.
- Reimer PJ, Hughen KA, Guilderson TP, McCormac G, Baillie MGL, Bard E, Barratt P, Beck JW, Buck CE, Damon PE, Friedrich M, Kromer B, Bronk Ramsey C, Reimer RW, Remmele S, Southon JR, Stuiver M, van der Plicht J. 2002. Preliminary report of the first workshop of the IntCal04 Radiocarbon Calibration/Comparison Working Group. *Radiocarbon* 44(3):653–61.
- Reimer PJ, Brown TA, Reimer RW. 2004. Discussion: reporting and calibration of post-bomb  $^{14}\text{C}$  data. *Radiocarbon* 46(3):1299–304.
- Reimer PJ, Baillie MGL, Bard E, Bayliss A, Beck JW, Blackwell PG, Bronk Ramsey C, Buck CE, Burr GS, Edwards RL, Friedrich M, Grootes PM, Guilderson TP, Hajdas I, Heaton TJ, Hogg AG, Hughen KA, Kaiser KF, Kromer B, McCormac FG, Manning SW, Reimer RW, Richards DA, Southon JR, Talamo S, Turney CSM, van der Plicht J, Weyhenmeyer CE. 2009. IntCal09 and Marine09 radiocarbon age calibration curves, 0–50,000 years cal BP. *Radiocarbon* 51(4):1111–50.
- Slota PJ Jr, Jull AJT, Linick TW, Toolin LJ. 1987. Preparation of small samples for  $^{14}\text{C}$  accelerator targets by catalytic reduction of CO. *Radiocarbon* 29(2):303–6.
- Smith VC, Mark DF, Staff RA, Blockley SPE, Bronk Ramsey C, Bryant CL, Nakagawa T, Han KK, Weh A, Takemura K, Danhara T, Suigetsu 2006 Project Members. 2011. Toward establishing precise  $^{40}\text{Ar}/^{39}\text{Ar}$  chronologies for Late Pleistocene palaeoclimate archives: an example from the Lake Suigetsu (Japan) sedimentary record. *Quaternary Science Reviews*. doi:10.1016/j.quascirev.2011.06.020.
- Staff RA. 2011. Research on radiocarbon calibration records, focussing on new measurements from Lake Suigetsu, Japan [unpublished DPhil thesis]. University of Oxford.
- Staff RA, Bronk Ramsey C, Bryant CL, Brock F, Lamb HF, Marshall MH, Brauer A, Schlolaut G, Tarasov P, Payne RL, Pearson EJ, Yokoyama Y, Tyler J, Haraguchi T, Gotanda K, Yonenobu H, Nakagawa T. 2009. Suigetsu 2006: a wholly terrestrial radiocarbon calibration curve. Paper presented at the 20th International Radiocarbon Conference, 31 May–5 June 2009. Kona, Hawaii.
- Staff RA, Bronk Ramsey C, Nakagawa T, Suigetsu 2006 Project Members. 2010. A re-analysis of the Lake Suigetsu terrestrial radiocarbon dataset. *Nuclear Instruments and Methods in Physics Research B* 268(7–8):960–5.
- Stuiver M. 1982. A high-precision calibration of the AD radiocarbon timescale. *Radiocarbon* 24(1):1–26.
- Stuiver M, Polach HA. 1977. Discussion: reporting of  $^{14}\text{C}$  data. *Radiocarbon* 19(3):355–63.
- Stuiver M, Reimer PJ. 1993. Extended  $^{14}\text{C}$  data base and revised CALIB 3.0  $^{14}\text{C}$  age calibration program. *Radiocarbon* 35(1):215–30.
- Suess HE. 1970. The three causes of secular C14 fluctuations, their amplitudes and time constants. In: Olsson IU, editor. *Radiocarbon Variations and Absolute Chronology; Twelfth Nobel Symposium, Uppsala 1969*. New York: John Wiley and Sons. p 595–605.
- van der Plicht J, Beck JW, Bard E, Baillie MGL, Blackwell PG, Buck CE, Friedrich M, Guilderson TP, Hughen KA, Kromer B, McCormac FG, Bronk Ramsey C, Reimer PJ, Reimer RW, Remmele S, Richards DA, Southon JR, Stuiver M, Weyhenmeyer CE. 2004. NotCal04—comparison/calibration  $^{14}\text{C}$  records 26–50 cal kyr BP. *Radiocarbon* 46(3):1225–38.
- Vogel JS, Southon JR, Nelson DE, Brown TA. 1984. Performance of catalytically condensed carbon for use in accelerator mass spectrometry. *Nuclear Instruments and Methods in Physics Research B* 5(2):289–93.
- Walker MJC. 2005. *Quaternary Dating Methods*. Chichester: John Wiley & Sons Ltd.
- Walker M, Johnsen S, Rasmussen SO, Popp T, Steffensen J-P, Gibbard P, Hoek W, Lowe J, Andrews J, Björck S, Cwynar L, Hughen K, Kershaw P, Kromer B, Litt T, Lowe DJ, Nakagawa T, Newnham R, Schwander J. 2009. Formal definition and dating of the GSSP (Global Stratotype Section and Point) for the base of the Holocene using the Greenland NGRIP ice core, and selected auxiliary records. *Journal of Quaternary Science* 24(1):3–17.
- Xu S, Anderson R, Bryant C, Cook GT, Dougans A, Freeman S, Naysmith P, Schnabel C, Scott EM. 2004. Capabilities of the new SUERC 5MV AMS facility for  $^{14}\text{C}$  dating. *Radiocarbon* 46(1):59–64.

**APPENDIX 1**

A truncated version of the OxCal `P_Sequence` model coding applied for the Poisson process deposition modeling of the Lake Suigetsu (SG06)  $^{14}\text{C}$  data on to the IntCal09 calibration curve (Reimer et al. 2009).

```
Options()
{ Resolution=1; Curve="IntCal09"; };
Plot()
{
  Outlier_Model("Default", T(5), U(0,4), "r");
  P_Sequence("Core top to 1500 cm composite depth", 2)
  {
    Boundary("1500 cm composite depth")
    { color="Gray"; z=1477.0; };
    R_F14C("oxA-24502", 0.27585, 0.00161)
    { Outlier(0.05); color="Blue"; z=1473.2; };
    R_F14C("oxA-24503", 0.27387, 0.00144)
    { Outlier(0.05); color="Blue"; z=1472.3; };
    R_F14C("SUERC-17726", 0.28296, 0.00162)
    { Outlier(0.05); color="DeepPink"; z=1472.2; };
    R_F14C("oxA-24499", 0.27514, 0.00159)
    { Outlier(0.05); color="Blue"; z=1465.9; };
    R_F14C("oxA-24500", 0.27285, 0.00252)
    { Outlier(0.05); color="Blue"; z=1461.7; };

    etc...

    R_F14C("SUERC-18130", 0.28166, 0.00159)
    { Outlier(0.05); color="DeepPink"; z=1432.6; };
    R_Combine("OxA-24448/OxA-24449")
    { R_F14C("oxA-24448", 0.28675, 0.00177)
      { Outlier(0.05); color="Blue"; };
      R_F14C("oxA-24449", 0.28597, 0.00176)
      { Outlier(0.05); color="Blue"; };
      Outlier(0.05); color="Blue"; z=1428.6; };
    R_F14C("SUERC-29832", 0.28566, 0.00136)
    { Outlier(0.05); color="DeepPink"; z=1425; };

    etc...

    Date("Holocene onset")
    { color="Green"; z=1413.4; };

    etc...

    Date("SG06-1288 tephra")
    { color="Gray"; z=1273.4; };

    etc...

    Boundary("175 cm event-free depth")
    { color="Gray"; z=175.0; };

    etc...

    Boundary("SG06 core top", U(calBP(750), calBP(-50)))
    { color="Gray"; z=20.0; };
  };
};
```



APPENDIX 2

The 182 <sup>14</sup>C determinations of terrestrial plant macrofossil samples picked from the upper 15 m (composite depth) of the SG06 sediment core (92 from ORAU and 90 from NRCF-E).

Appendix 2

SG06 macro-fossil sample ID	Sample type <sup>a</sup>	Composite depth (cm) (ver. 24 Aug 2009)	Event-free depth (cm) (Jan 2011)	AMS target ID	Conventional <sup>14</sup> C age BP (±1 σ) (Stuiver and Polach 1977)	F <sup>14</sup> C (±1 σ) (Reimer et al. 2004)	Modeled, calibrated age (IntCal09 cal yr BP) (68.2% range)	Posterior outlier probability (%)
1209	D.B.L.	1496.2	1473.2	OxA-24502	10,346 ± 47	0.27585 ± 0.00161	12,269–12,178	2
1210 & 1211	D.B.L.	1495.3	1472.3	OxA-24503	10,404 ± 42	0.27387 ± 0.00144	12,260–12,169	1
135	D.B.L.	1495.2	1472.2	SUERC-17726	10,141 ± 46	0.28296 ± 0.00162	12,258–12,169	100
1206	D.B.L.	1488.9	1465.9	OxA-24499	10,366 ± 46	0.27514 ± 0.00159	12,189–12,120	1
1207	D.B.L.	1484.7	1461.7	OxA-24500	10,433 ± 74	0.27285 ± 0.00252	12,150–12,086	3
133	D.B.L.	1479.1	1456.1	OxA-24273	10,329 ± 42	0.27643 ± 0.00143	12,095–12,039	2
112	D.B.L.	1475.2	1452.2	OxA-24193	10,285 ± 42	0.27793 ± 0.00147	12,055–11,998	2
1208	D.B.L.	1471.1	1448.1	OxA-24501	10,211 ± 40	0.28050 ± 0.00138	12,013–11,957	1
1152	D.B.L.	1467.6	1444.6	OxA-24433	10,249 ± 42	0.27918 ± 0.00146	11,977–11,918	3
109	D.B.L.	1460.3	1437.3	OxA-24250	10,202 ± 45	0.28082 ± 0.00158	11,881–11,839	1
1150	D.B.L.	1459.2	1436.2	SUERC-29862	10,324 ± 40	0.27661 ± 0.00136	11,867–11,829	42
108	D.B.L.	1457.1	1434.1	SUERC-23750	10,110 ± 77	0.28407 ± 0.00271	11,845–11,800	2
107	D.B.L.	1455.6	1432.6	SUERC-18130	10,178 ± 45	0.28166 ± 0.00159	11,830–11,781	1
1149	D.B.L.	1451.6	1428.6	OxA-24448	10,034 ± 50	0.28675 ± 0.00177	11,797–11,733	3
1149	D.B.L.	1451.6	1428.6	OxA-24449	10,056 ± 49	0.28597 ± 0.00176	11,797–11,733	2
1151	D.B.L.	1448.0	1425.0	SUERC-29832	10,065 ± 38	0.28566 ± 0.00136	11,757–11,692	2
105	D.B.L.	1444.3	1421.3	OxA-24292	9992 ± 64	0.28826 ± 0.00230	11,730–11,645	4
1155	D.B.L.	1444.2	1421.2	SUERC-29831	10,112 ± 40	0.28399 ± 0.00140	11,729–11,644	1
1147	D.B.L.	1443.2	1420.2	SUERC-29830	10,120 ± 39	0.28372 ± 0.00137	11,720–11,631	2
103	D.B.L.	1440.6	1417.6	SUERC-20491	10,014 ± 45	0.28748 ± 0.00161	11,699–11,599	2
102	D.B.L.	1433.7	1410.7	OxA-24196	10,124 ± 50	0.28358 ± 0.00177	11,638–11,518	4
101	D.B.L.	1433.5	1410.5	SUERC-23746	10,054 ± 75	0.28606 ± 0.00265	11,636–11,516	2
660	D.B.L.	1429.0	1408.3	OxA-24468	9962 ± 93	0.28934 ± 0.00336	11,613–11,499	2
1159	Twig	1424.9	1404.2	OxA-24455	9941 ± 56	0.29012 ± 0.00201	11,571–11,460	3
099	D.B.L.	1420.7	1400.0	OxA-24200	10,080 ± 55	0.28511 ± 0.00197	11,525–11,418	1
1158	D.B.L.	1420.7	1400.0	SUERC-29521	10,094 ± 41	0.28464 ± 0.00147	11,525–11,418	3
097	D.B.L.	1408.7	1388.0	SUERC-19061	6968 ± 94	0.42004 ± 0.00494	11,383–11,322	100
1146	D.B.L.	1400.9	1380.2	OxA-24446	9884 ± 50	0.29216 ± 0.00181	11,291–11,249	1
1146	D.B.L.	1400.9	1380.2	OxA-24447	9872 ± 49	0.29260 ± 0.00180	11,291–11,249	2
094	D.B.L.	1394.9	1374.2	SUERC-17115	9817 ± 50	0.29463 ± 0.00183	11,230–11,203	2
093	D.B.L.	1394.3	1373.6	SUERC-17717	9755 ± 44	0.29691 ± 0.00162	11,225–11,197	2
1121	Twig	1383.2	1362.5	OxA-24431	9672 ± 40	0.30000 ± 0.00149	11,123–11,094	1
1121	Twig	1383.2	1362.5	OxA-24432	9678 ± 39	0.29976 ± 0.00145	11,123–11,094	1
092	Twig	1383.1	1362.4	SUERC-20490	9642 ± 42	0.30111 ± 0.00156	11,122–11,093	1
1120	D.B.L.	1378.4	1357.7	OxA-24445	9554 ± 46	0.30443 ± 0.00173	11,075–11,043	1
1125	Twig	1372.2	1351.5	SUERC-29520	9600 ± 38	0.30270 ± 0.00144	11,020–10,980	1
1119	D.B.L.	1365.1	1344.4	SUERC-29519	9699 ± 38	0.29896 ± 0.00142	10,944–10,908	10
659	D.B.L.	1361.4	1340.7	OxA-24310	9598 ± 43	0.30277 ± 0.00163	10,911–10,871	1
088	D.B.L.	1354.5	1334.4	SUERC-17721	9550 ± 50	0.30457 ± 0.00191	10,860–10,817	1
086	D.B.L.	1351.6	1331.5	SUERC-20489	9549 ± 43	0.30461 ± 0.00164	10,834–10,790	1
658	D.B.L.	1345.1	1325.0	OxA-24367	9547 ± 39	0.30468 ± 0.00148	10,777–10,736	1
1118	D.B.L.	1335.6	1315.5	SUERC-29518	9460 ± 37	0.30799 ± 0.00142	10,690–10,652	2
083	D.B.L.	1329.1	1309.0	SUERC-17120	9442 ± 45	0.30868 ± 0.00174	10,622–10,586	2
081	D.B.L.	1317.4	1297.3	OxA-24207	9235 ± 52	0.31677 ± 0.00206	10,496–10,459	2

## Appendix 2 (Continued)

SG06 macro- fossil sample ID	Sample type <sup>a</sup>	Composite depth (cm) (ver. 24 Aug 2009)	Event- free depth (cm) (ver. 29 Jan 2011)	AMS target ID	Conventional <sup>14</sup> C age BP (±1 σ) (Stuiver and Polach 1977)	F <sup>14</sup> C (±1 σ) (Reimer et al. 2004)	Modeled, calibrated age (IntCal09 cal yr BP) (68.2% range)	Posterior outlier proba- bility (%)
1123	D.B.L.	1314.0	1293.9	SUERC-29517	9334 ± 42	0.31287 ± 0.00162	10,459–10,425	4
1128	D.B.L.	1306.2	1286.1	SUERC-29516	9286 ± 37	0.31475 ± 0.00145	10,380–10,331	6
079	E.B.L.	1299.2	1279.1	OxA-24239	9137 ± 40	0.32066 ± 0.00161	10,287–10,255	2
078	D.B.L.	1298.9	1278.8	OxA-24187	9161 ± 38	0.31970 ± 0.00153	10,283–10,252	1
843	D.B.L.	1288.8	1274.2	SUERC-26732	9024 ± 39	0.32519 ± 0.00157	10,236–10,210	6
842	D.B.L.	1274.3	1261.6	OxA-24391	8874 ± 46	0.33131 ± 0.00189	10,142–10,095	1
438	D.B.L.	1260.8	1248.1	OxA-24291	8946 ± 43	0.32836 ± 0.00174	10,048–9967	2
848	D.B.L.	1260.1	1247.4	SUERC-29513	8951 ± 38	0.32814 ± 0.00157	10,044–9961	2
847	D.B.L.	1259.6	1246.9	OxA-24440	8870 ± 47	0.33147 ± 0.00195	10,037–9956	2
847	D.B.L.	1259.6	1246.9	SUERC-28906	8730 ± 45	0.33732 ± 0.00191	10,037–9956	61
076	D.B.L.	1257.7	1245.0	SUERC-16524	8512 ± 71	0.34656 ± 0.00308	10,006–9945	100
075	Twig	1234.1	1221.4	SUERC-17118	8751 ± 43	0.33643 ± 0.00180	9809–9756	2
441	D.B.L.	1233.6	1220.9	OxA-24309	8845 ± 41	0.33251 ± 0.00171	9804–9753	2
439	D.B.L.	1229.3	1216.6	SUERC-25995	8825 ± 38	0.33335 ± 0.00158	9764–9711	2
878	D.B.L.	1225.2	1212.5	OxA-24329	8774 ± 46	0.33547 ± 0.00194	9727–9682	1
442	D.B.L.	1207.9	1195.2	OxA-24425	8563 ± 40	0.34438 ± 0.00172	9551–9529	5
877	D.B.L.	1198.0	1185.3	OxA-24420	8439 ± 38	0.34973 ± 0.00165	9483–9454	1
444	D.B.L.	1198.0	1185.3	SUERC-26366	8422 ± 40	0.35047 ± 0.00173	9483–9454	1
070	D.B.L.	1180.8	1168.1	OxA-24192	8362 ± 37	0.35310 ± 0.00161	9354–9320	1
874	D.B.L.	1176.2	1163.5	SUERC-27503	8406 ± 47	0.35119 ± 0.00206	9320–9283	12
069	D.B.L.	1164.6	1151.9	OxA-24280	8306 ± 42	0.35558 ± 0.00188	9212–9164	4
068	D.B.L.	1156.9	1144.2	SUERC-20486	8158 ± 38	0.36218 ± 0.00172	9135–9098	2
067	D.B.L.	1143.6	1130.9	OxA-24249	8096 ± 39	0.36500 ± 0.00178	9022–8996	4
065	E.B.L.	1130.3	1117.6	OxA-24288	8081 ± 35	0.36568 ± 0.00157	8907–8863	23
063	D.B.L.	1121.9	1109.2	OxA-24259	8107 ± 39	0.36450 ± 0.00179	8823–8780	49
024	E.B.L.	1103.6	1090.9	SUERC-18129	7766 ± 41	0.38029 ± 0.00192	8626–8569	4
629	E.B.L.	1097.9	1085.2	OxA-24424	7739 ± 41	0.38159 ± 0.00193	8565–8518	1
629	E.B.L.	1097.9	1085.2	SUERC-28229	7781 ± 38	0.37962 ± 0.00180	8565–8518	2
630	E.B.L.	1095.8	1083.1	OxA-24366	7775 ± 35	0.37987 ± 0.00167	8552–8487	2
382	D.B.L.	1077.5	1064.8	OxA-X-2297-53	7878 ± 41	0.37506 ± 0.00193	8347–8314	100
061	D.B.L.	1076.6	1063.9	SUERC-20485	7407 ± 38	0.39771 ± 0.00190	8336–8307	3
060	E.B.L.	1074.6	1061.9	OxA-24246	7375 ± 36	0.39928 ± 0.00178	8318–8290	5
059	D.B.L.	1064.6	1051.9	SUERC-20484	7503 ± 41	0.39297 ± 0.00199	8240–8218	2
383	D.B.L.	1063.4	1050.7	OxA-24287	7500 ± 35	0.39309 ± 0.00169	8231–8210	3
058	D.B.L.	1056.8	1044.1	OxA-24322	7334 ± 37	0.40132 ± 0.00187	8181–8156	1
057	D.B.L.	1049.7	1038.4	SUERC-20482	7345 ± 41	0.40079 ± 0.00203	8139–8104	2
381	D.B.L.	1043.6	1032.3	OxA-24267	7284 ± 37	0.40381 ± 0.00188	8089–8046	1
381	D.B.L.	1043.6	1032.3	OxA-24268	7269 ± 38	0.40457 ± 0.00192	8089–8046	1
055	D.B.L.	1032.1	1020.8	SUERC-23358	7120 ± 48	0.41217 ± 0.00245	7992–7954	2
384	D.B.L.	1029.2	1017.9	OxA-24286	7171 ± 34	0.40957 ± 0.00172	7969–7934	12
054	E.B.L.	1019.9	1008.6	SUERC-17725	6951 ± 39	0.42092 ± 0.00205	7865–7816	3
387	D.B.L.	1016.2	1004.9	OxA-24272	7091 ± 35	0.41367 ± 0.00179	7845–7773	45
638	E.B.L.	1007.3	996.0	SUERC-25994	6956 ± 40	0.42068 ± 0.00212	7724–7684	4
052	E.B.L.	998.0	986.7	SUERC-20481	6650 ± 39	0.43701 ± 0.00213	7606–7557	9
433	D.B.L.	990.3	979.0	OxA-24419	6630 ± 34	0.43810 ± 0.00184	7521–7486	1
433	D.B.L.	990.3	979.0	SUERC-28207	6715 ± 47	0.43349 ± 0.00252	7521–7486	8
051	D.B.L.	987.3	976.0	OxA-24245	6477 ± 34	0.44651 ± 0.00191	7484–7452	28
435	E.B.L.	983.8	972.5	SUERC-26365	6558 ± 37	0.44202 ± 0.00203	7450–7425	6
050	E.B.L.	969.8	958.5	SUERC-17117	6129 ± 38	0.46626 ± 0.00218	7299–7226	87
429	E.B.L.	960.5	952.0	OxA-X-2339-40	6042 ± 34	0.47133 ± 0.00201	7230–7131	83
428	D.B.L.	957.1	948.6	SUERC-25993	6216 ± 35	0.46126 ± 0.00202	7183–7096	2
047	D.B.L.	939.0	930.5	OxA-24279	6096 ± 35	0.46818 ± 0.00205	6992–6935	1

Appendix 2 (Continued)

SG06 macro- fossil sample ID	Sample type <sup>a</sup>	Composite depth (cm) (ver. 24 Aug 2009)	Event- free depth (cm) (ver. 29 Jan 2011)	AMS target ID	Conventional <sup>14</sup> C age BP (±1 σ) (Stuiver and Polach 1977)	F <sup>14</sup> C (±1 σ) (Reimer et al. 2004)	Modeled, calibrated age (IntCal09 cal yr BP) (68.2% range)	Posterior outlier proba- bility (%)
046	E.B.L.	925.7	917.2	SUERC-20480	6035 ± 40	0.47176 ± 0.00237	6850–6792	2
043	D.B.L.	906.6	898.1	SUERC-26731	5783 ± 38	0.48677 ± 0.00232	6634–6581	1
041	D.B.L.	898.1	889.6	OxA-24255	5717 ± 31	0.49081 ± 0.00191	6535–6485	1
039	E.B.L.	876.9	869.2	OxA-24181	5500 ± 34	0.50427 ± 0.00211	6298–6282	1
039	E.B.L.	876.9	869.2	OxA-24182	5458 ± 35	0.50688 ± 0.00218	6298–6282	1
039	E.B.L.	876.9	869.2	SUERC-13332	5465 ± 35	0.50647 ± 0.00220	6298–6282	1
038	D.B.L.	861.0	853.3	SUERC-23355	5320 ± 38	0.51567 ± 0.00244	6181–6137	1
037	E.B.L.	854.9	847.2	OxA-24262	5332 ± 33	0.51488 ± 0.00210	6129–6071	1
480	E.B.L.	839.9	832.2	SUERC-26362	5230 ± 38	0.52150 ± 0.00246	5994–5952	1
777	E.B.L.	820.6	812.9	SUERC-28228	5048 ± 38	0.53342 ± 0.00252	5828–5788	1
036	D.B.L.	812.0	804.3	SUERC-20479	4962 ± 35	0.53917 ± 0.00235	5748–5722	5
479	E.B.L.	800.8	793.1	SUERC-25992	4974 ± 35	0.53838 ± 0.00235	5672–5647	1
023	Bark	792.7	785.0	OxA-24220	4862 ± 30	0.54591 ± 0.00206	5604–5588	2
782	E.B.L.	780.0	772.3	SUERC-28206	4883 ± 38	0.54454 ± 0.00255	5503–5488	16
780	E.B.L.	773.0	765.3	OxA-24351	4848 ± 35	0.54687 ± 0.00240	5448–5426	97
780	E.B.L.	773.0	765.3	SUERC-28203	4625 ± 35	0.56227 ± 0.00248	5448–5426	4
779	D.B.L.	768.1	760.4	SUERC-28202	4729 ± 39	0.55506 ± 0.00272	5415–5392	3
488	E.B.L.	761.8	754.1	SUERC-25990	4773 ± 37	0.55203 ± 0.00255	5375–5341	5
016	E.B.L.	754.1	746.4	OxA-24238	4655 ± 34	0.56021 ± 0.00238	5326–5304	19
786	D.B.L.	748.3	740.6	OxA-X-2360-44	4427 ± 32	0.57631 ± 0.00229	5273–5243	4
015	Bark	738.0	730.3	SUERC-23354	4595 ± 38	0.56442 ± 0.00264	5180–5143	11
508	Bark	713.5	707.1	SUERC-25989	4486 ± 35	0.57209 ± 0.00249	4997–4974	5
014	Twig	705.8	699.4	OxA-24285	4388 ± 29	0.57915 ± 0.00208	4933–4900	1
013	D.B.L.	693.7	687.3	OxA-24195	4136 ± 34	0.59754 ± 0.00251	4822–4798	2
012	D.B.L.	691.9	685.5	SUERC-20476	4166 ± 37	0.59533 ± 0.00277	4808–4784	1
008	E.B.L.	685.4	679.0	OxA-24284	4211 ± 28	0.59203 ± 0.00209	4758–4731	2
007	E.B.L.	678.2	671.8	SUERC-26730	4241 ± 37	0.58980 ± 0.00274	4718–4656	8
511	E.B.L.	667.9	661.5	SUERC-26361	4235 ± 37	0.59025 ± 0.00274	4638–4578	34
006	E.B.L.	657.6	651.2	OxA-24271	4009 ± 28	0.60710 ± 0.00215	4567–4496	4
513	E.B.L.	653.4	647.0	SUERC-25988	4041 ± 37	0.60472 ± 0.00278	4527–4461	1
004	E.B.L.	635.2	628.8	OxA-24277	3895 ± 29	0.61575 ± 0.00225	4392–4338	1
004	E.B.L.	635.2	628.8	OxA-24278	3923 ± 30	0.61364 ± 0.00227	4392–4338	1
002	E.B.L.	631.6	625.2	OxA-24237	3906 ± 31	0.61497 ± 0.00238	4367–4303	1
003	E.B.L.	631.6	625.2	SUERC-23353	3982 ± 36	0.60915 ± 0.00270	4367–4303	12
005	E.B.L.	616.0	609.6	SUERC-20475	3806 ± 37	0.62263 ± 0.00289	4245–4206	1
608	D.B.L.	602.1	595.7	SUERC-26360	3700 ± 37	0.63091 ± 0.00293	4148–4125	2
326	D.B.L.	596.0	589.6	OxA-24194	3815 ± 28	0.62192 ± 0.00216	4110–4089	21
325	E.B.L.	579.4	573.0	SUERC-20474	3650 ± 35	0.63484 ± 0.00278	3983–3938	1
606	E.B.L.	571.8	565.4	OxA-24321	3620 ± 30	0.63724 ± 0.00239	3921–3874	1
503	E.B.L.	561.3	554.9	SUERC-25985	3527 ± 37	0.64463 ± 0.00297	3835–3778	1
504	E.B.L.	548.9	542.5	OxA-24300	3436 ± 30	0.65197 ± 0.00244	3721–3681	1
323	E.B.L.	535.0	528.6	SUERC-20473	3340 ± 37	0.65985 ± 0.00305	3606–3562	1
604	E.B.L.	527.5	521.1	SUERC-28201	3331 ± 37	0.66057 ± 0.00308	3543–3497	1
603	E.B.L.	508.4	502.0	OxA-24320	3152 ± 28	0.67543 ± 0.00233	3387–3352	2
322	E.B.L.	500.4	494.0	SUERC-26729	3251 ± 36	0.66715 ± 0.00302	3320–3272	98
321	E.B.L.	484.7	478.3	OxA-24232	2943 ± 27	0.69322 ± 0.00234	3200–3123	1
492	D.B.L.	477.5	471.1	SUERC-28200	2952 ± 38	0.69249 ± 0.00323	3128–3061	1
320	E.B.L.	461.6	455.2	OxA-24308	2964 ± 30	0.69141 ± 0.00258	3010–2896	67
493	E.B.L.	449.4	443.0	SUERC-26359	2760 ± 37	0.70926 ± 0.00328	2849–2779	1
319	E.B.L.	439.9	433.5	OxA-X-2297-56	2493 ± 25	0.73321 ± 0.00229	2721–2686	1
319	E.B.L.	439.9	433.5	OxA-X-2303-36	2487 ± 27	0.73374 ± 0.00247	2721–2686	1
318	E.B.L.	428.4	422.0	SUERC-23360	2514 ± 35	0.73124 ± 0.00320	2639–2585	1

## Appendix 2 (Continued)

SG06 macro- fossil sample ID	Sample type <sup>a</sup>	Composite depth (cm) (ver. 24 Aug 2009)	Event- free depth (cm) (ver. 29 Jan 2011)	AMS target ID	Conventional <sup>14</sup> C age BP (±1 σ) (Stuiver and Polach 1977)	F <sup>14</sup> C (±1 σ) (Reimer et al. 2004)	Modeled, calibrated age (IntCal09 cal yr BP) (68.2% range)	Posterior outlier proba- bility (%)
022	E.B.L.	413.9	407.5	OxA-24235	2426 ± 25	0.73934 ± 0.00230	2537–2471	7
022	E.B.L.	413.9	407.5	OxA-24236	2489 ± 26	0.73356 ± 0.00235	2537–2471	1
021	E.B.L.	413.9	407.5	SUERC-20472	2499 ± 37	0.73260 ± 0.00338	2537–2471	1
317	E.B.L.	406.3	399.9	OxA-24183	2483 ± 28	0.73408 ± 0.00258	2478–2404	3
317	E.B.L.	406.3	399.9	SUERC-13335	2456 ± 35	0.73655 ± 0.00320	2478–2404	1
562	D.B.L.	399.0	392.6	SUERC-25984	2411 ± 37	0.74074 ± 0.00340	2429–2350	1
528	D.B.L.	392.9	386.5	OxA-X-2347-43	2227 ± 24	0.75789 ± 0.00222	2388–2297	31
529	D.B.L.	387.3	380.9	SUERC-26358	2308 ± 35	0.75030 ± 0.00329	2351–2246	27
316	E.B.L.	369.0	362.6	OxA-24243	2109 ± 27	0.76908 ± 0.00259	2209–2104	2
316	E.B.L.	369.0	362.6	OxA-24244	2123 ± 27	0.76774 ± 0.00261	2209–2104	1
566	D.B.L.	362.7	356.3	SUERC-25983	2256 ± 37	0.75513 ± 0.00347	2167–2061	70
583	E.B.L.	344.6	338.2	SUERC-26357	2046 ± 35	0.77511 ± 0.00340	1995–1933	2
581	E.B.L.	337.0	330.6	OxA-24319	1915 ± 26	0.78793 ± 0.00259	1930–1874	10
315	E.B.L.	321.7	315.3	SUERC-20499	1944 ± 37	0.78506 ± 0.00359	1841–1777	14
556	E.B.L.	307.2	300.8	OxA-24379	1744 ± 24	0.80482 ± 0.00238	1712–1687	2
556	E.B.L.	307.2	300.8	SUERC-26728	1775 ± 35	0.80178 ± 0.00349	1712–1687	1
559	E.B.L.	298.8	292.4	SUERC-25982	1809 ± 37	0.79832 ± 0.00366	1652–1624	5
625	D.B.L.	290.6	284.2	OxA-24299	1798 ± 29	0.79942 ± 0.00284	1594–1555	60
624	E.B.L.	269.4	263.0	SUERC-26356	1535 ± 35	0.82602 ± 0.00363	1416–1383	1
389	E.B.L.	263.4	257.0	OxA-24266	1445 ± 26	0.83539 ± 0.00269	1369–1334	1
554	E.B.L.	251.8	245.4	SUERC-25981	1344 ± 35	0.84597 ± 0.00369	1288–1241	3
313	E.B.L.	233.9	227.5	OxA-24233	1251 ± 22	0.85582 ± 0.00236	1129–1082	5
390	E.B.L.	222.5	216.1	SUERC-23361	1125 ± 35	0.86932 ± 0.00379	1019–982	1
312	Twig	211.8	205.4	OxA-24191	927 ± 24	0.89098 ± 0.00268	919–894	2
310	E.B.L.	177.6	176.8	SUERC-20471	757 ± 37	0.91007 ± 0.00414	689–666	3
623	D.B.L.	152.0	152.0	SUERC-26355	694 ± 35	0.91722 ± 0.00402	583–566	4
308	Twig	136.4	136.4	OxA-X-2270-49	436 ± 25	0.94715 ± 0.00293	530–499	19
622	D.B.L.	113.8	113.8	SUERC-26727	457 ± 35	0.94469 ± 0.00412	475–381	42
307	E.B.L.	108.4	108.4	OxA-X-2248-48	730 ± 24	0.91309 ± 0.00274	460–355	74
307	E.B.L.	108.4	108.4	OxA-24231	505 ± 23	0.93908 ± 0.00273	460–355	45
621	D.B.L.	103.6	103.6	SUERC-25980	406 ± 35	0.95074 ± 0.00414	445–333	7
305	D.B.L.	67.5	67.5	OxA-24276	259 ± 24	0.96829 ± 0.00294	317–157	12
696	E.B.L.	42.0	42.0	OxA-24328	96 ± 27	0.98812 ± 0.00333	249–56	2
696	E.B.L.	42.0	42.0	SUERC-26724	136 ± 37	0.98319 ± 0.00452	249–56	1

<sup>a</sup>Sample types “D.B.L.” and “E.B.L.” refer to deciduous broad leaves and evergreen broad leaves, respectively.